Bull Soc Chim Fr (1995) 132, 1047-1051

Computer simulations of the low temperature oxidation of formaldehyde in oxygen-poor mixtures

Vincente Viossat[1], Marcel Vanpee[2], Jeanine Chamboux-Crosnier[3], Krikor Sahetchian[3]

[1] *Laboratoire de chimie générale, Université Pierre-et-Marie-Curie, Tour 54-55, 4, place Jussieu, 75252 Paris Cedex 05, France*
[2] *Department of Chemical Engineering, University of Massachusetts, Amherst, MA 01003, USA*
[3] *Laboratoire de mécanique physique (groupe de cinétique chimique), URA 879, 2, place de la Gare de Ceinture, 78210 Saint-Cyr-l'École, France*

(received 1st February 1995, accepted 28 July 1995)

Summary – This paper describes computer simulations of experiments on the low temperature oxidation of formaldehyde (from 643 to 705 K) for oxygen-poor mixtures. The reaction rate changes abruptly when the oxygen is completely consumed. A mechanism that explains this phenomenon and models the low temperature oxidation of formaldehyde is presented. In the presence of oxygen, the formaldehyde is consumed according to a degenerate branched chain reaction involving HO_2 radicals and H_2O_2; once the oxygen is consumed, the reaction proceeds *via* a mechanism of linear chains initiated by the decomposition of H_2O_2. From the proposed mechanism, simulated curves (product evolution, pressure change and temperature) have been obtained in good agreement with experimental curves, for different temperatures and equivalence ratios.

computer simulation / oxidation of formaldehyde

Introduction

Formaldehyde is an important intermediate in the combustion of hydrocarbons, especially methane. Much work has been devoted to the combustion of the formaldehyde [1-7]; some experiments have been analyzed numerically by using kinetic mechanisms [3, 5-7]. In the low temperature oxidation (from 643 to 705 K) of mixtures containing less than 33.3% oxygen, an interesting phenomenon was found by one of us [2a,d]. The evolution of the reaction changes abruptly when the oxygen is consumed; from this moment on the rate of formation of the reaction products increases. This behavior has been interpreted as the result of the formation of an intermediate peroxide which, when the oxygen has disappeared, induces the pyrolysis of formaldehyde [2a,d].

From the present knowledge of the kinetics of formaldehyde oxidation, we propose a reaction mechanism involving two groups of elementary reactions, which explains the observed phenomenon.

Experimental results

The experimental results presented in this section were obtained by Vanpee [2a,d]. We rapidly describe them here to compare with present results obtained by simulation.

The experiments were performed in a closed Pyrex vessel of cylindrical shape ($V = 270$ cm^3, $r = 2.3$ cm). The gaseous mixture was rapidly admitted to the empty vessel and the reaction occurred at constant volume. The reaction evolution was detected simultaneously by temperature and pressure changes. The temperature change ΔT was measured by a tungsten wire, which is a part of a Wheatstone bridge. The pressure change ΔP was measured by a glass membrane differential gauge. The two curves T and ΔP were simultaneously recorded *versus* time. The reaction products were analyzed according to a procedure described in reference [2c].

The experimental curves analyzed numerically in this work correspond to the following mixtures: CH_2O/O_2: 11:1; 8.1:1; 7.5:1; 1:1 (equivalence ratio: ($\Phi \geqslant 1$) and for temperatures between 643 and 705 K.

Figure 1a shows the ΔP and T curves registered for the mixture CH_2O/O_2: 11:1 at $T = 705$ K and $P = 53.4$ torr. The original curves given in reference [2d] have been modified (axes and scales) for an easier comparison between experimental and calculated curves. The ΔP and T curves change continuously until both curves break at time $\tau = 37$ s.

The same behavior was observed for all mixtures where the concentration of formaldehyde exceeds the stoichiometric composition ($\Phi > 1$). For example, when $CH_2O/O_2 = 7.5:1$ (fig 1b), the break occurs at time $\tau = 165$ s. On the other hand, when $\Phi \leqslant 1$, the curves do not show any discontinuity (fig 1c).

In another experiment (fig 2a), the analysis of the reaction products showed that the discontinuity occurs when the oxygen is consumed. From this time, hydrogen starts to be formed in appreciable amounts and the formation of carbon monoxide increases.

In the original papers [2a,d], a great number of experiments were performed. The same kinetic laws were always observed but the reproducibility of ΔP and T curves was not perfect, indicating a wall effect on the rate of the reaction.

In summary, the observations shown in figures 1a, 1b and 2a indicate two different regimes in the evolution of the reaction when $\Phi > 1$: a) as long as oxygen is present in the system, the evolution is similar to that of oxygen-poor mixtures ($\Phi < 1$); and b) when the consumption of oxygen is quasi-complete, the rate of disappearance of formaldehyde increases. The transition between the two regimes occurs when the discontinuity on the T, ΔP, $[H_2]$ and $[CO]$ curves is observed.

It should be noted that the break in the ΔP and T curves was also observed in the oxidation of methyl alcohol [8]. However, hydrocarbon oxidation does not show such an anomaly, as indicated in a review paper [8] where the oxidation of ethane, propane, butane, isobutane, ethylene and propylene were investigated.

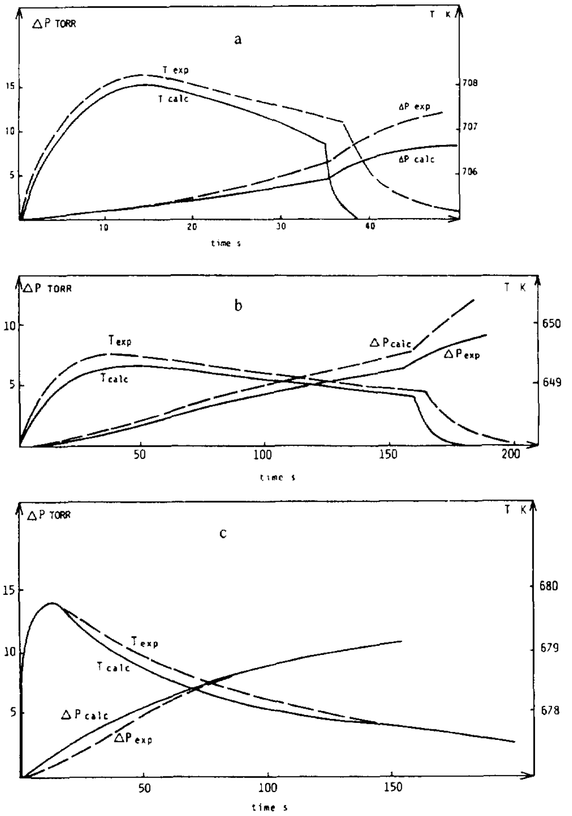

Fig 1. Oxidation of different mixtures computed (lines) and experimental data (dotted line). a) Mixture: 11.1 CH_2O + O_2. Initial pressure: 53.4 torr; initial temperature: 705 K. b) Mixture: 7.5 CH_2O + O_2. Initial pressure: 68.2 torr; initial temperature: 648 K. c) Mixture: CH_2O + O_2. Initial pressure: 111 torr; initial temperature: 677 K.

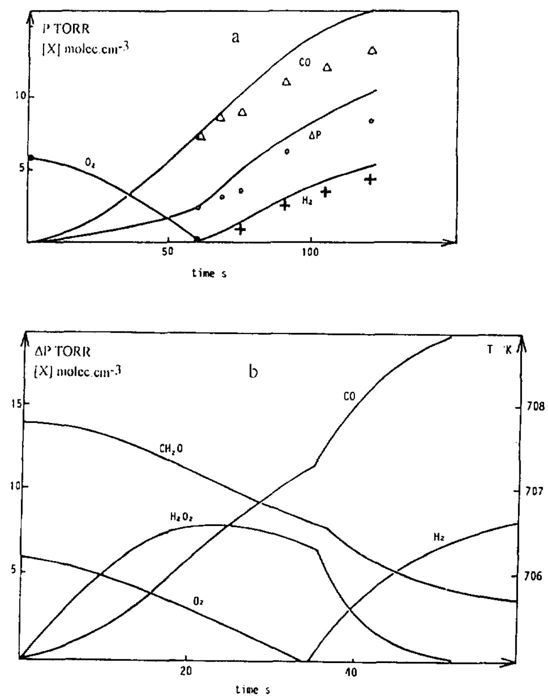

Fig 2. Evolution of the concentrations of species: a) Oxidation of mixture: 8.1 CH_2O + O_2. Initial pressure: 51.9 torr; initial temperature: 643 K. Computed (lines) and experimental data (symbols): Δ: CO; +: H_2; •: O_2; o: ΔP. b) Oxidation of mixture: 11.1 CH_2O + O_2. Initial pressure: 53.4 torr; initial temperature: 705 K. Computed concentration of the species: [X]: concentration (molecule × cm^{-3}), $[O_2] = [X] \times 10^{16}$; $[CH_2O] = [X] \times 5 \times 10^{16}$; $[H_2O_2] = [X] \times 10^{15}$; $[CO] = [X] \times 10^{16}$; $[H_2] = [X] \times 10^{16}$.

Study of the processes by numerical simulation

The evolution of species concentrations and temperature *versus* time can be examined by the resolution of a differential equation system, according to the Gear's method [9, 10]. The input data are: a reaction mechanism with rate constants for each elementary step; the thermochemical data and the thermal conductivities; the Nusselt number; and the characteristics of the reactor.

The variation of pressure is expressed by:

$$\Delta P = RT \sum_i [X_i] - P_o$$

where $[X_i]$ designates the concentration of the species i, P_o the initial pressure, and R the universal gas constant. The value of ΔP is therefore calculated from the values of the concentrations.

The temperature change in reactor *versus* time is calculated on the basis of the thermal balance:

$$\rho C_v V \, dT/dt = VQv - \beta S(T - T_o) \qquad (1)$$

ρ: specific mass of gas
C_v: specific heat at constant volume

V: volume of reactor
Q: heat of reaction at a constant volume
v: reaction rate
S: inside surface of reactor
β: coefficient of heat transfer between gas and walls of the reactor = Nu (λ/r)
λ: thermal conductivity
r: radius of the cylindrical reactor
Nu: Nusselt number

For the reaction mixture equation (1) becomes:

$$\sum_i \rho_i C_{vi} V \frac{dT}{dt} = V \sum_i Q_i v_i - \frac{\mathrm{Nu}}{\mathrm{r}} \lambda_{\mathrm{mix}} S(T - T_o)$$

The conductivity of the multicomponent mixture (λ_{mix}) is calculated in a subroutine program according to the formula of Mason and Saxena [11]. The value of the Nusselt number is obtained by zeroing dT/dt in equation (1) in such a way as to reproduce the maximum experimental value of T (Nu = 1.5). Q_i is obtained from the enthalpies [12].

Table I lists the rate constants chosen in the literature for the set of selected reactions [13-18].

This is a low temperature reaction mechanism in which the chain carriers are the free radicals HCO, HO_2, OH and H. At temperatures below 773 K, the concentration of atomic oxygen is exceedingly low, less than 10^4 atoms per cm^3. The reactions of atomic oxygen are therefore entirely negligible and have been omitted in the reaction scheme.

The following elementary reactions have been shown to have a negligible influence on the overall rate (the overall rate is $\sum_i v_i$) and have been neglected:

$H + HO_2 = OH + OH$	$k = 2.8 \times 10^{-10} \exp(-440/T)$	[14]
$H + HO_2 = H_2 + O_2$	$k = 1.1 \times 10^{-10} \exp(-1\,070/T)$	[14]
$OH + HO_2 = H_2O + O_2$	$k = 2.4 \times 10^{-8} T^{-1}$	[14]
$HO_2 + CO \rightarrow CO_2 + OH$	$k = 2.5 \times 10^{-10} \exp(-11\,900/T)$	[14]
$H + CO + M \rightarrow HCO + M$	$k = 10^{-33}$	[18]
$H + O_2 + M \rightarrow HO_2 + M$	$k = 10^{-32}$	[18]

The importance of each elementary reaction can be tested by the influence of the variation of its rate constant on the overall rate of the reaction. For instance, a change of rate constants k_3 and k_5 has a great influence on the position of the break in the T and ΔP curves, *ie* on the rate of reaction in the presence of oxygen. To be able to reproduce the experimental value of τ, we must introduce the heterogeneous reactions 12 and 13, which are also necessary reactions to balance the pressure variation. The rate coefficients of these reactions have been adjusted in order to obtain the best agreement with experiment, *ie* a better fit for the values of τ and ΔP. This procedure is reasonable since the physical state of the reaction vessel walls can change from one experiment to another, probably because the walls were not treated.

The values of k_{12} and k_{13} mainly influence the slow reaction preceding the break. Their values are given in table I.

A change of k_4 acts essentially on the position of the maximum temperature. After the break, reactions 7, 8 and 9 have a great influence on the value of ΔP. Thus, they affect the CO and H_2 production, *ie* the rate of the reaction in the absence of oxygen.

The reaction HCO + HCO affects ΔP and ΔT after the break for the mixtures ($\Phi > 1$). The literature gives the value of k_{15} at 300 K. To reproduce the experimental results, we have fitted this rate constant between 643 and 705 K. The selected values lead to the expression: $k_{15} = 1.6 \times 10^{-11} \exp{(880 \pm 200)/T}$.

After verifying that some reactions have an important role as long as oxygen is present (*ie* before the discontinuity in the ΔP and T curves) and that others dominate in the absence of oxygen (after the discontinuity), we propose one group of reactions (labelled *Group I* in table I) for the mechanism of consumption of formaldehyde in the presence of oxygen, and a second group (labelled *Group II*) for the decomposition of formaldehyde in the absence of oxygen.

From the global scheme (table I), simulations have been performed (fig 1a, 1b, 1c and 2a) corresponding to the experimental curves. For the conditions corresponding to figures 1a, b, c, the experimental product evolution has not been determined. It would be interesting to simulate their evolution in order to illustrate the two oxidation regimes (fig 2b).

The reactions and rate constants have been chosen to match: the time τ corresponding to the discontinuity; the shape of the ΔP, T, $[O_2]$, $[H_2]$ and [CO] curves, and the position of the maximum temperature; and the order of magnitude of variations in temperature and pressure. The best fit is obtained if we slightly modify the values of some of the rate constants. The values of the modified rate constants selected for our computations (k_3, k_4, k_7, k_8, k_{15}) are given in table I. These values fall within the limits of accuracy given by the authors. The agreement between the calculated and the experimental curves is satisfactory.

The experimental curves indicate two regimes of reaction, one in the presence of oxygen, the other in the absence of oxygen, and so it is of interest to verify that only the *Group I* reactions determine the first regime and only the *Group II* reactions determine the second. For instance, for the conditions of figure 1a, the curves are calculated by using the *Group I* reactions before the discontinuity, and the *Group II* reactions after it. For the computation of *Group II* curves, the initial time is the discontinuity time. The initial concentrations are those calculated at the discontinuity. The curves obtained (fig 3) are superimposed on the calculated curves of figures 1a and 2b, calculated with the entire reaction scheme.

The transition between the two regimes of reaction is due to the competition between reactions 2 and 7. The rate constant of reaction 2 is about 1 000 times greater than that of reaction 7, and so as long as oxygen is present the HCO radical will be converted into

Table I

Group	Reactions	Literature expression	f*	Ref	Rate Constants (s, cm^3, molecule) Literature values 705 K	677 K	648 K	643 K	This work 705 K	677 K	648 K	643 K
	1. $H_2CO + O_2 \rightarrow HCO + HO_2$	$7.50 \times 10^{-11} e^{-20634/T}$		[13]	1.5×10^{-23}	4.3×10^{-24}	1.1×10^{-24}	8.7×10^{-25}		Literature		
	2. $HCO + O_2 \rightarrow CO + HO_2$	$7.97 \times 10^{-12} e^{-120/T}$		[15]	6.7×10^{-12}	6.7×10^{-12}	6.6×10^{-12}	6.6×10^{-12}		Literature		
I	3. $HO_2 + H_2CO \rightarrow H_2O_2 + HCO$	$1.16 \times 10^{-11} e^{-6160/T}$	3	[15]	1.9×10^{-15}	1.3×10^{-15}	8.6×10^{-16}	8.0×10^{-16}	3.9×10^{-15}	2.7×10^{-15}	2×10^{-15}	2×10^{-15}
	4. $HO_2 + HO_2 \rightarrow H_2O_2 + O_2$	$6.98 \times 10^{-10} e^{-6030/T}$ +		[15]	8.3×10^{-13}	8.2×10^{-13}	8.3×10^{-13}	8.3×10^{-13}	1.1×10^{-12}	1.0×10^{-12}	1.0×10^{-12}	1.0×10^{-12}
		$2.16 \times 10^{-13} e^{+820/T}$										
	5. $H_2O_2 + M \rightarrow OH + OH + M)$)	$2.66 \times 10^{-8} e^{-21640/T}$		[16]	1.2×10^{-21}	3.5×10^{-22}	8.3×10^{-23}	6.4×10^{-23}		Literature		
	6. $H + H_2O_2 \rightarrow H_2 + HO_2$	$2.82 \times 10^{-12} e^{-1880/T}$		[17]	2.0×10^{-13}	1.7×10^{-13}	1.5×10^{-13}	1.5×10^{-13}		Literature		
	7. $HCO + M \rightarrow H + CO + M$	$4.15 \times 10^{-10} e^{-8456/T}$	2	[17]	2.6×10^{-15}	1.6×10^{-15}	8.9×10^{-16}	8.1×10^{-16}	3.7×10^{-15}	2.3×10^{-15}	1.3×10^{-15}	1.2×10^{-15}
	8. $H + H_2CO \rightarrow H_2 + HCO$	$9.63 \times 10^{-11} e^{-2280/T}$	1.3	[15]	3.8×10^{-12}	3.3×10^{-12}	2.8×10^{-12}	2.8×10^{-12}	5.9×10^{-12}	5.2×10^{-12}	4.4×10^{-12}	4.4×10^{-12}
II	9. $HCO + H \rightarrow H_2 + CO$	3.32×10^{-10}		[17]	3.3×10^{-10}	3.3×10^{-10}	3.3×10^{-10}	3.3×10^{-10}		Literature		
	10. $OH + H_2CO \rightarrow H_2O + HCO$	$4.32 \times 10^{-11} e^{-400/T}$	2	[15]	2.4×10^{-11}	2.4×10^{-11}	2.3×10^{-11}	2.3×10^{-11}		Literature		
	11. $OH + H_2O_2 \rightarrow H_2O + O_2$	$1.16 \times 10^{-11} e^{-722/T}$		[17]	4.2×10^{-12}	4.0×10^{-12}	3.8×10^{-12}	3.8×10^{-12}		Literature		
I	12. $HO_2 \rightarrow 1/2\ H_2O + 3/4\ O_2$		1.5						5.0	4.5	0.25	0.1
	13. $H_2O_2 \rightarrow 1/2\ O_2 + H_2O$								0.65	0.6	0.12	0.06
	14. $HO_2 + HCO \rightarrow CO_2 + OH + H$	5.0×10^{-11}		[14]	5.0×10^{-11}	5.0×10^{-11}	5.0×10^{-11}	5.0×10^{-11}		Literature		
	15. $HCO + HCO \rightarrow H_2 + CO$	5.0×10^{-11} (300 K)	2	[18]					0.4×10^{-11}		0.75×10^{-11}	0.8×10^{-11}

* f: uncertainty factor; I: *Group I*; II: *Group II*.

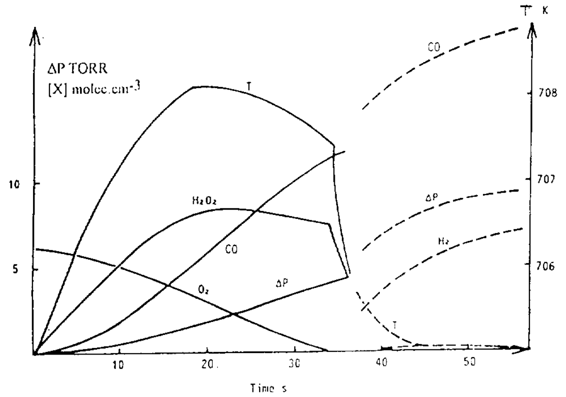

Fig 3. Computed data for oxidation of mixture: 11.1 CH_2O + O_2 at P = 53.4 torr and T = 705 K. ——— Curves calculated with reactions of *Group I*. ------- Curves calculated with reactions of *Group II*.

HO_2 through reaction 2 and therefore favors the oxidation process. It is only when all the oxygen has been consumed that HCO can dissociate (according to reaction 7) to permit the development of the chain process by which H_2CO is converted to H_2 and CO. The sharpness of the transition is due to the magnitude of the ratio of the two rate constants k_2/k_7. It is of interest to note that the occurrence of the break is by no means due to a spurious effect of the reactor's walls. If we set k_{12} and k_{13} equal to zero, the mechanism proposed still predicts the existence of a sharp transition between two regimes. However, as we explained previously, k_{12} and k_{13} affect the magnitude of the pressure variations and the position of the break.

Finally, to better illustrate the mechanism of the process, table II presents the calculated free radical concentrations at different times in the reaction process for the experiment corresponding to figure 1a, and the rates V_3, V_8, V_{10}, which lead to the formaldehyde consumption. At $\tau = 20$ s, the oxidation regime is found. At this stage, HO_2 has the highest concentration among the free radicals and is responsible, through reaction 3, for the majority of the formaldehyde consumption. At $\tau = 37$ s the pyrolysis regime occurs. Here, the H concentration has increased and reaction 8, which involves atomic hydrogen, becomes responsible for the consumption of H_2CO. This process continues until all the hydrogen peroxide has disappeared.

Conclusion

We have proposed two groups of reactions which allow the simulation of the formaldehyde oxidation in oxygen-poor mixtures. The reaction occurs by two consecutive paths: a degenerate branching chain reaction followed by an induced pyrolysis. These results explain the abrupt discontinuity observed in the reaction rate at low temperature in oxygen-poor mixture conditions.

Table II. Free radical concentrations (calculated) and rates of formaldehyde conversion in the oxidation of a formaldehyde oxygen-poor mixture CH_2O/O_2: 11:1; initial pressure: 53.4 torr; initial temperature: 705 K.

	Concentration, molecules/cm^3		
Species	t = 20 s	t = 34 s	t = 37 s
HO_2	1.69×10^{12}	1.22×10^{12}	5.11×10^{11}
HCO	2.38×10^{10}	1.50×10^{11}	5.39×10^{11}
OH	1.05×10^{6}	1.36×10^{6}	1.53×10^{6}
H	8.16×10^{7}	5.84×10^{8}	2.2×10^{9}

	Rate of formaldehyde conversion, molecules/cm$^3 \cdot s^{-1}$		
Rate	t = 20 s	t = 34 s	t = 37 s
V (total)	2.12×10^{15}	2.46×10^{15}	4.93×10^{15}
V_3	1.93×10^{15}	1.26×10^{15}	5.14×10^{14}
V_8	1.87×10^{14}	1.20×10^{15}	4.43×10^{15}
V_{10}	1.52×10^{13}	1.78×10^{13}	1.94×10^{13}

V_i: rate of formaldehyde conversion through reaction i.

References

1 Axford DWE, Norrish RGW, *Proc Roy Soc A* (1948) 192, 518

2 a) Vanpee M, *Bull Soc Chim Belg* (1953) 62, 285
b) Vanpee M, *CR Acad Sci, Paris* (1955) 241, 951
c) Vanpee M, *CR Acad Sci, Paris* (1956) 242, 373
d) Vanpee M, Thèse Louvain (1956)

3 Vardanyan I, Sahetchian K, Nalbandyan AB, *Combust Flame* (1971) 17, 315; (1974) 22, 153

4 Minkoff GY, Tipper GFH, *Chemistry of Combustion Reactions*, Butterworks, London, 1962

5 Vandooren J, Oldenhove de Guertechin L, van Tiggelen PJ, *Combust Flame* (1986) 64, 127

6 Olsson JO, Olsson IBM, *J Phys Chem* (1989) 93, 3107

7 Hochgreb S, Yetter RA, Dryer SL, 23rd Int Symposium on Combustion (1991) 171

8 Vanpee M, *Bull Soc Chim Belg* (1953) 62, 468

9 Gear CW, *Comm Ach* (1971) 14, 175 and 185

10 Boettner JC, Cathonnet M, Dagault P, Gaillard F, *Mathematical Modelling in Combustion and Related Topics*, Brauner CIM, Smidt Laine, Eds, Nijhoff, 1988; Nato Series E Appl Sc, vol 140, p 421

11 Mason EA, Saxena SC, *Phys Fluids* (1958) 1, 361

12 Benson SW, *Fundations of Chemical Kinetics*, McGraw-Hill, New York, 1960

13 Vardanyan I, Sachyan GA, Nalbandyan AB, *Int J Chem Kinet* (1975) 7, 23

14 Tsang W, Hampson RF, *J Phys Chem Ref Data* (1986) 15, 1087

15 Hippler H, Troe J, Willner J, *J Chem Phys* (1990) 93 (3), 1775

16 Kijewki H, Troe J-J, *Helv Chem Acta* (1972) 55, 205

17 Fontijn A, Clyne MAA, *Reactions of Small Transient Species* (1983), Academic, London

18 Baulch DL, Cobos CJ, Cox RA, Esser C, Frank P, Just Th, Kerr JA, Pilling MJ, Troe J, Walker RW, Wamatz J, *J Phys Chem Ref Data* (1992) 21, (3), 411